AN ABSTRACT OF THE THESIS OF

VERNON C. NEWTON III for the degree MASTER OF SCIENCE
(Name) (Degree)

in CIVIL ENGINEERING presented on June 13, 1974
(Major Department) (Date)

Title: ULTIMATE BEARING CAPACITY OF SHALLOW FOOTINGS ON PLASTIC SILT Redacted for privacy

Abstract approved: J. R. Bell

The usual approach to calculation of the ultimate bearing capacity of plastic silt is to assume no porewater drainage occurs during the loading period. The coefficient of permeability of plastic silt is generally significantly larger than clay; therefore, partial drainage of porewater may occur during the loading period. This study evaluates the validity of the no porewater drainage assumption as it applies to a particular plastic silt.

A series of plate load tests were performed on three circular footings of different sizes, placed on the bottom of a shallow excavation. Ultimate bearing capacity for each footing is interpreted from load-settlement curves. Samples were taken from the test pit and the shear strength was evaluated by laboratory testing. The shear strength is used in the Terzaghi, Meyerhof, and Hansen bearing capacity equations. Bearing capacities calculated using the no

porewater drainage assumption and local shear failure conditions yield the best correlation with load test data.

Ultimate Bearing Capacity of Shallow Footings on Plastic Silt

by

Vernon C. Newton III

A THESIS

submitted to

Oregon State University

in partial fulfillment of
the requirements for the
degree of

Master of Science

Completed June 1974

Commencement June 1975

APPROVED:

Redacted for privacy

Professor of Civil Engineering
in charge of major

Redacted for privacy

Head of Department of Civil Engineering

Redacted for privacy

Dean of Graduate School

Date thesis is presented June 13, 1974

Typed by Mary Jo Stratton for Vernon C. Newton III

ACKNOWLEDGEMENTS

The author wishes to express gratitude to Dr. J. R. Bell for his encouragement, advice, and assistance in developing a testing scheme, interpreting data, and thesis preparation. He is also indebted to Dr. W. L. Schroeder for advice concerning testing procedures and data inrepretation.

Acknowledgement is due to the Oregon State University Department of Civil Engineering for funding this study.

Special thanks to my wife, Janice, for encouraging me to pursue graduate study and for her assistance in typing the rough draft of this thesis.

TABLE OF CONTENTS

	Page
I. INTRODUCTION	1
II. PURPOSE AND SCOPE	3
III. LITERATURE REVIEW	4
The Nature of Ultimate Bearing Capacity	4
General Bearing Capacity Equations	6
Bearing Capacity of Cohesive Soil	11
IV. TESTING SCHEME	14
V. FIELD TESTS	17
Apparatus	17
Procedure	21
Results	23
VI. SOIL PROPERTIES	30
Soil Testing	30
Results	32
VII. INTERPRETATION OF RESULTS	39
VIII. CONCLUSIONS	48
BIBLIOGRAPHY	49

LIST OF TABLES

Table		Page
1	Summary of Undrained Soil Strength.	35
2	Comparison of Methods of Determining Ultimate Bearing Capacity from Load Test Data.	41
3	Calculated Bearing Capacity Compared to Load Test Results.	45

LIST OF FIGURES

Figure		Page
1	Typical and Idealized Load-Settlement Curves.	5
2	Models for Bearing Capacity Equations.	7
3	Load Test Arrangement.	18
4	Test Site Layout.	19
5	Dial Gage Extensometer Installation.	22
6	Load-Settlement Curve (1 ft^2 circular footing).	24
7	Load-Settlement Curve (2 ft^2 circular footing).	25
8	Load-Settlement Curve (3 ft^2 circular footing).	26
9	Comparison of Average Footing Contact Pressure versus Settlement for Various Footing Areas.	28
10	Average Footing Contact Pressure versus Settlement in the Last 5 Minutes.	29
11	Soil Profile at Test Site.	33
12	Location of Strength Tests Performed on Samples from the Test Site.	34
13	Void Ratio versus Log Effective Stress.	36
14	Dial Reading versus Log Time Curve (1/2 TSF load).	37

SYMBOLS

B (ft)	= one-half the width of a strip footing
c (lbs/ft^2)	= apparent soil cohesion
d_c (dimensionless)	= depth factor with respect to cohesion applied to the general bearing capacity equation
D_f (ft)	= vertical distance between the ground surface and the base of the footing
d_q (dimensionless)	= depth factor with respect to surcharge applied to the general bearing capacity equation
d_γ (dimensionless)	= depth factor with respect to soil weight applied to the general bearing capacity equation
N_c (dimensionless)	= bearing capacity factor with respect to cohesion
N_q (dimensionless)	= bearing capacity factor with respect to surcharge
N_γ (dimensionless)	= bearing capacity factor with respect to soil weight
q_D (lbs/ft^2)	= ultimate bearing capacity per unit area
s_c (dimensionless)	= shape factor with respect to cohesion applied to the general bearing capacity equation
s_q (dimensionless)	= shape factor with respect to surcharge applied to the general bearing capacity equation
s_γ (dimensionless)	= shape factor with respect to soil weight applied to the general bearing capacity equation
t_{100} (minutes)	= time required for 100 percent of primary consolidation
γ (lbs/ft^3)	= unit weight of soil
ϕ (degrees)	= angle of internal friction
ψ (degrees)	= angle

ULTIMATE BEARING CAPACITY OF SHALLOW FOOTINGS ON PLASTIC SILT

I. INTRODUCTION

Different assumptions are currently used in the calculation of ultimate bearing capacity, depending on whether the footing rests on cohesionless or cohesive soil. The difference in design procedures is based on whether or not drainage of excess porewater pressure takes place during the loading period. In the design of foundations for structures the loading period is generally taken as the time required to construct the structure. In general it is assumed that sands and gravels are freely draining. No drainage is presumed to take place in clays during the construction period. The free drainage assumption is valid for clean sands and gravels and the no drainage during loading assumption is valid for clays of low permeability. Many naturally occurring soils demonstrate intermediate drainage rates. These intermediate soils are generally silts. Silts may be further divided into two categories: those with the characteristics of ultra fine sand, and those that are cohesive or plastic. It has been suggested that the first category be treated as sands and the second category be treated as clays (18)[1]. This study deals with the validity of the no drainage

---

[1]Numbers in parentheses refer to items in the Bibliography.

assumption in assessing the ultimate bearing capacity of a particular plastic silt.

II. PURPOSE AND SCOPE

The purpose of this study is to examine the validity of the no porewater drainage assumption used to calculate the bearing capacity of plastic silts. The bearing capacities of a plastic silt determined from field load tests on three different sized footings will be compared to the bearing capacities calculated from laboratory strength tests and the Terzaghi general bearing capacity equation as modified by Meyerhof and Hansen. Conclusions will be made as to whether the bearing capacity measured in situ is best modeled by full, partial or no porewater drainage.

III. LITERATURE REVIEW

The Nature of Ultimate Bearing Capacity

The ultimate bearing capacity of a soil is defined by the maximum load per unit area which the soil can support without rupture (16). Prior to acceptance of the general bearing capacity equation, the ultimate bearing capacity of a soil was determined from load tests. Typical load tests results are presented in Figure 1 as a plot of load versus settlement. Case A is an idealized soil which shows elastic deformation up to the ultimate bearing capacity and perfectly plastic deformation for loads above the ultimate bearing capacity. Behavior of real soils never corresponds to this idealized model. Dense sands and stiff clays tend to yield load-settlement curves similar to Case B in Figure 1, while soft clays and loose sands yield curves similar to Case C (18). For Case B, if the initial straight line portion is extended forward and the final straight line portion is extended backward, the point where they intersect is often taken as the ultimate bearing capacity. Several procedures have been developed for evaluating the ultimate bearing capacity for load-settlement curves similar to Case C (7, 8).

Housel (7) has developed a procedure for determining bearing capacity of cohesive soils from load test data, where loads are applied

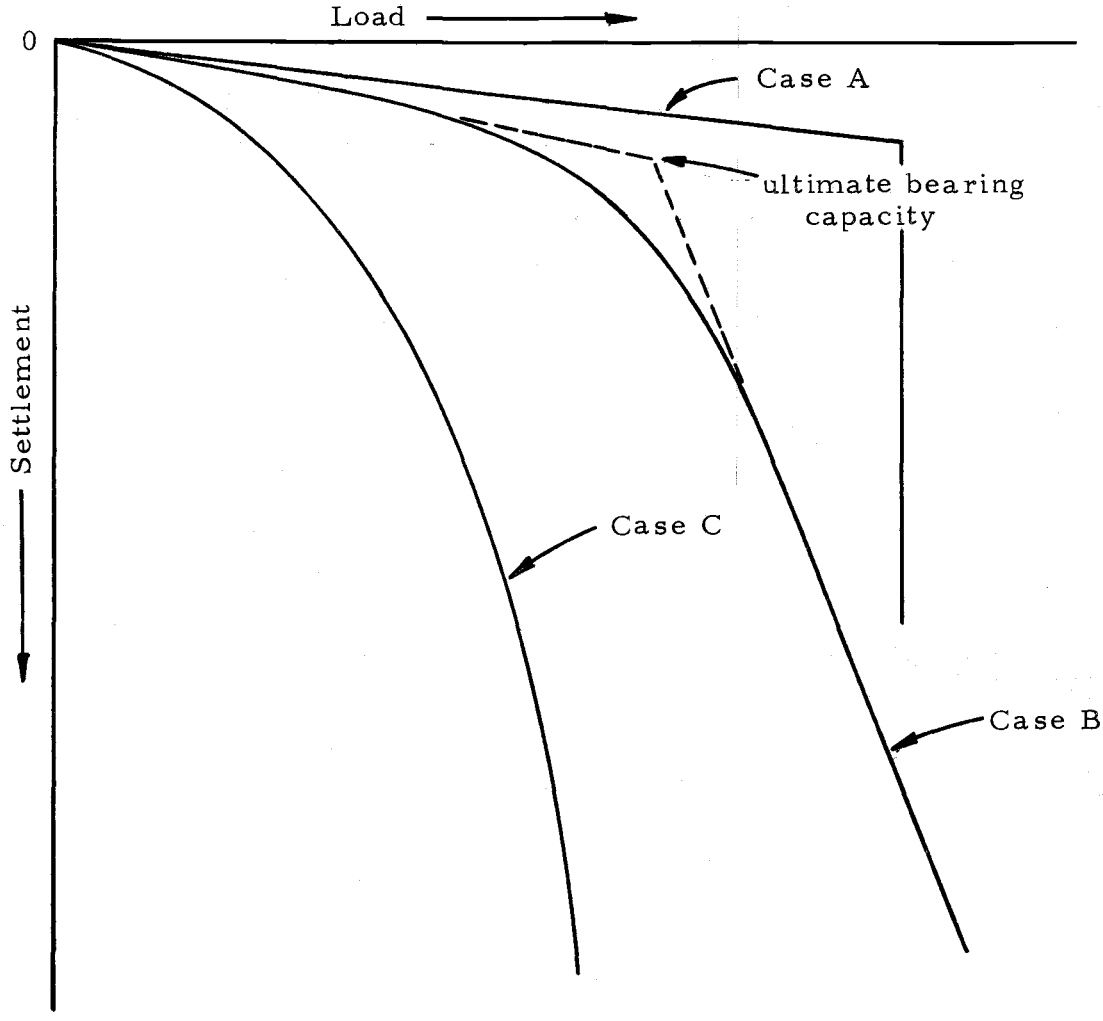

Figure 1. Typical and Idealized Load-Settlement Curves.

for one hour, and settlement in the last 30 minutes is plotted versus the average footing pressure. A distinct change in the slope of this curve indicates the ultimate bearing capacity.

Many soils, including the soil examined in this study (see Figures 6, 7 and 8 for load-settlement curves) do not show a sharp break in slope at the ultimate bearing capacity. The ultimate bearing capacity of a soil is not unique. It is deceiving to calculate an exact bearing capacity for a given soil, as variation due to the nonhomogeneity makes duplication of test results impossible. It is more proper to determine ranges of ultimate bearing capacity.

General Bearing Capacity Equations

Several ultimate bearing capacity theories have been developed. The general bearing capacity equation presented by Terzaghi and Peck (18) is based on work initiated by Prandtl in 1920. Prandtl's theory predicted the bearing capacity of an infinitely long footing of finite width. This type of footing is commonly referred to as a strip footing. The bottom of Prandtl's footing was smooth and rested on the soil surface. To simplify calculations, the soil was assumed to be a homogeneous, rigid, weightless material. The soil was confined by a uniform surcharge as shown in Figure 2a. In 1924, H. Reissner (17) wrote a differential equation for bearing capacity using Prandtl's

(a) The Prandtl Model

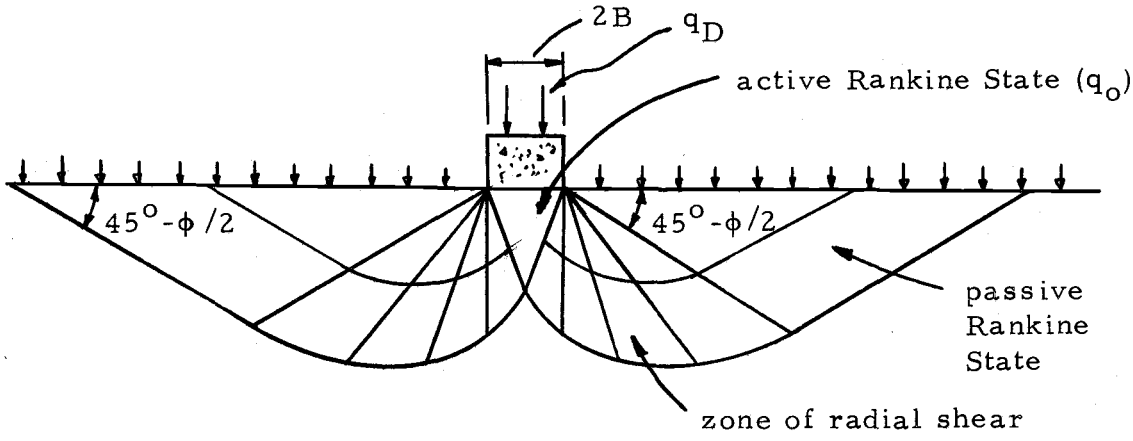

(b) The Terzaghi, Meyerhof Model

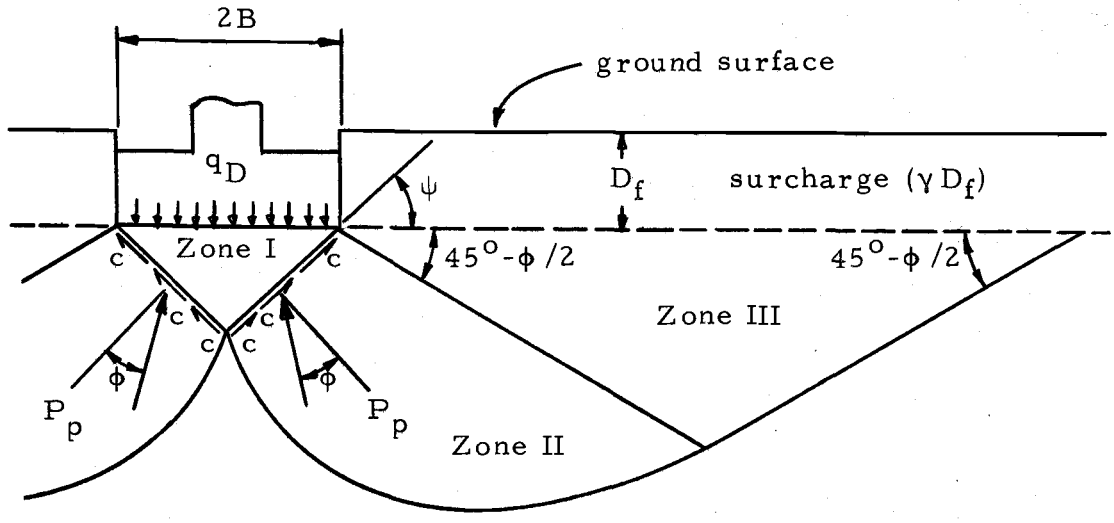

Figure 2. Models for Bearing Capacity Equations (15).

model, but including the effects of the soil weight. Unfortunately, no one has developed a rigorous solution to this equation.

In 1943, Terzaghi (17) presented the following bearing capacity equation:

$$q_D = cN_c + \gamma D_f N_q + \gamma BN_\gamma \quad [1]$$

where

q_D = ultimate bearing capacity per unit area,

B = 1/2 the footing width,

c = apparent soil cohesion,

D_f = vertical distance between the ground surface and the base of the footing,

γ = unit weight of the soil,

N_c = bearing capacity factor with respect to cohesion,

N_q = bearing capacity factor with respect to surcharge,

N_γ = bearing capacity factor with respect to soil weight.

Terzaghi obtained this approximate solution of Reissner's equation by making some simplifying assumptions. The soil above the base of the footing was replaced by an equivalent surcharge. Second, he assumed the curved portion of the failure surface followed a log spiral curve with the center of the curve at the edge of the footing. Figure 2b illustrates the Terzaghi bearing capacity model. The soil wedge, Zone I, is assumed to be a rigid extension of the footing. Lateral motion within the soil wedge is prevented by roughness of the

footing base and soil adhesion to the footing base. The soil in Zone II is in radial shear. It is forced downward and outward. The soil in Zone III is pushed upward and outward, so that passive earth pressure is mobilized. The three terms in the Terzaghi bearing capacity equation are the components of passive earth pressure due to cohesion, surcharge, and soil weight. The bearing capacity of the soil due to cohesion acting on the bottom of Zone I is also included in the passive earth pressure due to cohesion term. Then N_c, N_q, and N_γ depend only on ϕ, the angle of internal friction for the soil. Charts of values for N_c, N_q, and N_γ are available in several foundation engineering texts (3, 16, 17, 18).

Since the introduction of the Terzaghi general bearing capacity equation, Meyerhof (12) has suggested some improvements for its use, including revised N_c, N_q, and N_γ values. Meyerhof states that replacing the soil above the base of the footing with an equivalent surcharge leads to conservative values of bearing capacity. He suggests allowing the failure surface to extend above the footing base. Meyerhof also suggested that ψ in Figure 2b should be allowed to vary, rather than be held at ϕ. When ψ is varied, it is possible to determine a minimum bearing capacity. It is reasonable to expect the soil to fail along its weakest failure surface. These criteria were used when Meyerhof developed his N_c, N_q, and N_γ versus ϕ

relationships. Meyerhof also did extensive work in evaluating the bearing capacity of shapes other than the strip footing.

Brinch Hansen (3) also developed an expression for bearing capacity by applying shape and depth factors to the equation developed by Terzaghi. He used the Meyerhof values for N_c and N_q, but calculated N_γ from

$$N_\gamma = 1.80\ (N_q - 1) \tan \phi .$$

The Hansen equation for the bearing capacity of footings carrying vertical concentric loads is (3)

$$q_D = cN_c s_c d_c + \gamma D_f N_q s_q d_q + \gamma B N_\gamma s_\gamma d_\gamma \qquad [2]$$

where s_c, s_q, and s_γ are shape factors and d_c, d_q, and d_γ are depth factors.

In the practice of foundation engineering, the accepted procedure for calculating soil bearing capacity for shallow footings is to use some form of the Terzaghi general bearing capacity equation with shape factors and appropriate N_c, N_q, and N_γ factors. However, Terzaghi's bearing capacity equation is only valid when a general shear failure takes place. General shear failure occurs when all the soil strength along the failure surface is mobilized simultaneously. If the shearing strength of the soil is exceeded without the distinct failure surface being developed, then the failure is called a "local shear failure" and the theory is invalid. There is no rigorous bearing

capacity theory for local shear failure, but Terzaghi suggests the following empirical reductions (17):

use

$$c' = 2/3\ c$$

and

$$\tan \phi' = 2/3 \tan$$

then, the bearing capacity can be expressed by

$$q_D = c'N_c + \gamma D_f N'_q + \gamma B N'_\gamma \qquad [3]$$

where N'_c, N'_q, and N'_γ are N_c, N_q, and N_γ, determined using ϕ'.

Bearing Capacity of Cohesive Soil

The accepted procedure for determining bearing capacity of a cohesive soil is to assume no porewater drainage occurs. For saturated soil without drainage of porewater, the value of ϕ is zero. Therefore, the undrained case is commonly referred to as the $\phi = 0$ case. When ϕ equals zero, N_γ equals zero and N_q equals one. Therefore, the general bearing capacity equation is reduced to

$$q_D = cN_c s_c + \gamma D_f S_c \qquad [4]$$

For footings placed on the soil surface or on the bottom of an excavation, D_f becomes zero and this equation can be further reduced to

$$q_D = cN_c S_c \qquad [5]$$

For circular footings, applying the appropriate shape and bearing capacity factors soil bearing capacity equations by Terzaghi, Meyerhof, and Hansen become:

Terzaghi	$q_D = 6.17\ c$	[6a]
Meyerhof	$q_D = 6.18\ c$	[6b]
Hansen	$q_D = 6.68\ c$	[6c]

Numerous studies have compared the bearing capacity predicted for clay soils with the bearing capacity measured by load tests (2, 13, 15). In a study made by Skempton (15) it was found that Meyerhof's procedure for calculating bearing capacity showed close correlation with measured bearing capacity. D.M. Milovic (13) obtained the best correlation with measured bearing capacity of shallow footings on cohesive soil using Brinch Hansen's modifications to the Terzaghi equation. Field load tests performed by A. Berfelt (2) on plates of various shapes yielded ultimate bearing capacities that correlated well with values calculated using the Meyerhof procedure. The results of these studies indicate that the Meyerhof and Hansen procedures for calculating bearing capacity of cohesive soils provide the best evaluation of bearing capacity as measured in load tests.

The bearing capacity of a medium silt was examined at the State Institute for Technical Research, Finland (6). Medium silt is a MIT soil classification. A grain size versus percent finer curve was

presented for this soil and it indicates the soil is most likely non-plastic. The bearing capacity determined from plate load tests was arbitrarily designated as the footing pressure when 10 millimeters of settlement had occurred. No attempt was made to correlate bearing capacities measured with calculated bearing capacities. It was noted that the bearing capacity of this soil was sensitive to the length of the loading period.

IV. TESTING SCHEME

According to the references cited in the Literature Review (2, 3, 13, 15), the best determination of bearing capacity of cohesive soils was calculated using the Meyerhof or Hansen analysis. For vertical, concentric loads on circular footings at the soil surface, the bearing capacity equation is reduced to

$$q_D = cN_cS_c$$

The values for the Terzaghi, Meyerhof, and Hansen procedures are given as Equations 6a, 6b, and 6c. If the $\phi = 0$ case is valid for the silt considered in this study, then the bearing capacity calculated from the Meyerhof or Hansen analysis, using the cohesion determined from laboratory strength testing should be the bearing capacity measured in the load tests. For the $\phi = 0$ case, the bearing capacity of all the footings should be the same, as the footing size no longer appears in the bearing capacity equation. If these conditions are satisfied, then the $\phi = 0$ analysis is valid for the silt studied and the investigation is concluded.

However, if the bearing capacity calculated using the $\phi = 0$ analysis is smaller than the bearing capacity observed from the load tests and if the bearing capacity of the larger footings is greater than the bearing capacity of the smaller footings, then it would appear that

at least partial drainage of porewater had occurred during the loading period. In this case, the soil behaves as if ϕ is not equal to zero, then for circular footings on the soil surface and loaded with vertical, concentric loads, the bearing capacity equation is

$$q_D = cN_cS_c + \gamma BN_\gamma s_\gamma .$$

Load testing could supply q_D and B values and γ could be evaluated from soil properties measured in the laboratory. The bearing capacity factors N_c and N_γ are dependent upon ϕ ; therefore, there is one equation with two unknowns, ϕ and c. Load tests on two footings of different sizes would provide two independent equations to be written in terms of ϕ and c and, hence, both unknowns could be evaluated. Three footing sizes were used in this study to provide a check. The c and ϕ determined in this manner could then be compared to the c and ϕ determined for drained conditions in the laboratory to estimate the degree of drainage that had occurred in the field.

Several load test site conditions were required. First, it was necessary to locate a site where plastic silts could be found at shallow depths. The site was located on the Oregon State University campus where previous sampling and testing (4) had shown that plastic silt could be found at shallow depths. Second, to insure the possibility that the $\phi = 0$ case could develop in this soil, the soil under the footings had to be saturated. An observation well was

installed at the site and monitored. The load tests were performed after the water table had been observed near the ground surface for several months. Third, it was necessary to place the test footings at a depth in the soil profile below the "A" horizon so that organic matter and root systems would not affect the development of the failure surface. It is general practice in foundation engineering to locate all foundations below the depth of the "A" horizon; therefore, the tests were performed in the bottom of an 18 inch deep test pit. Fourth, in the test scheme, it was assumed that the surcharge term could be eliminated from the bearing capacity equation. To be sure that no surcharge was acting over the failure surface, the extent of the failure was estimated using data presented by Sowers (16) and the excavation was completed to the desired depth and extended beyond the estimated failure surface in each direction. The final condition was to find a site where the soil under one test footing was the same as the soil under the other test footings. The test site chosen was level and without any natural distinguishing land features. The soil at this site had a common sedimentary genesis.

V. FIELD TESTS

Apparatus

Load was applied to the footings with a 30 ton jack reacting against a truss anchored to the soil as shown in Figure 3. The pin connected truss was designed for a 50,000 pound capacity. The truss could be assembled and disassembled by two men. The arrangement of the test footings in the excavation and the location of the anchors is shown in Figure 4. The truss was anchored at two ends for the one- and two-square-foot footings. The three-square-foot footings required four anchors. The truss was constructed so that four inches of movement in each direction was provided for centering the truss over the test footings.

The anchors consisted of concrete blocks filling the bottom five feet of 20 inch diameter holes augered to depths of 10 feet. Two number five reinforcing bars were placed in each anchor block. One inch anchor bolts were threaded to allow one foot of vertical adjustment of the truss. The pullout resistance of the anchors was developed from skin friction on the concrete surface and the weight of the concrete. Each anchor was designed to exceed a pullout capacity of 12,500 pounds.

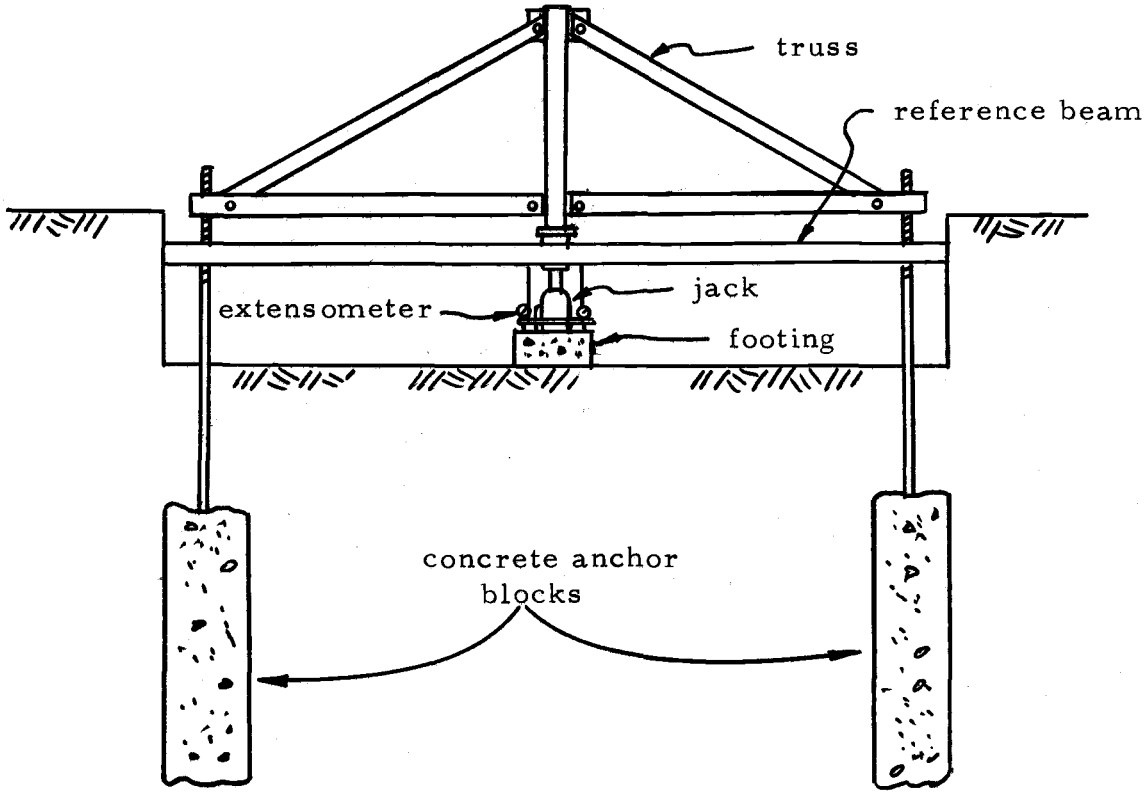

Schematic Section of Load Test Arrangement

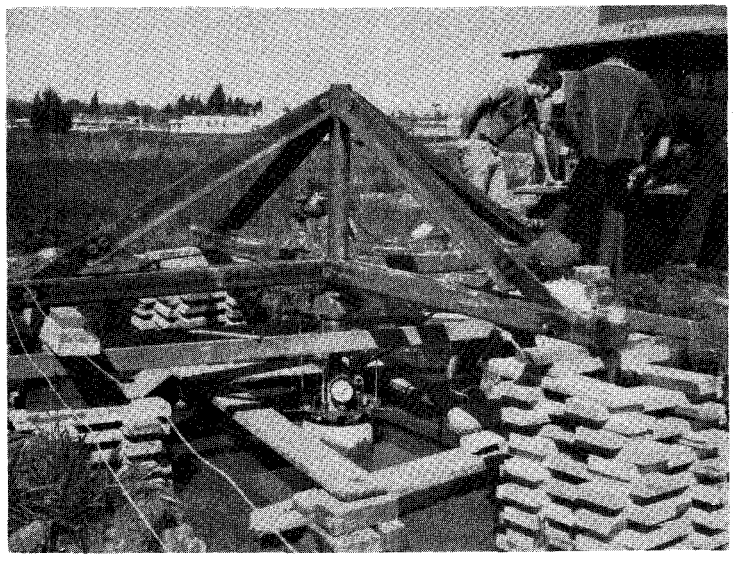

Figure 3. Load Test Arrangement.

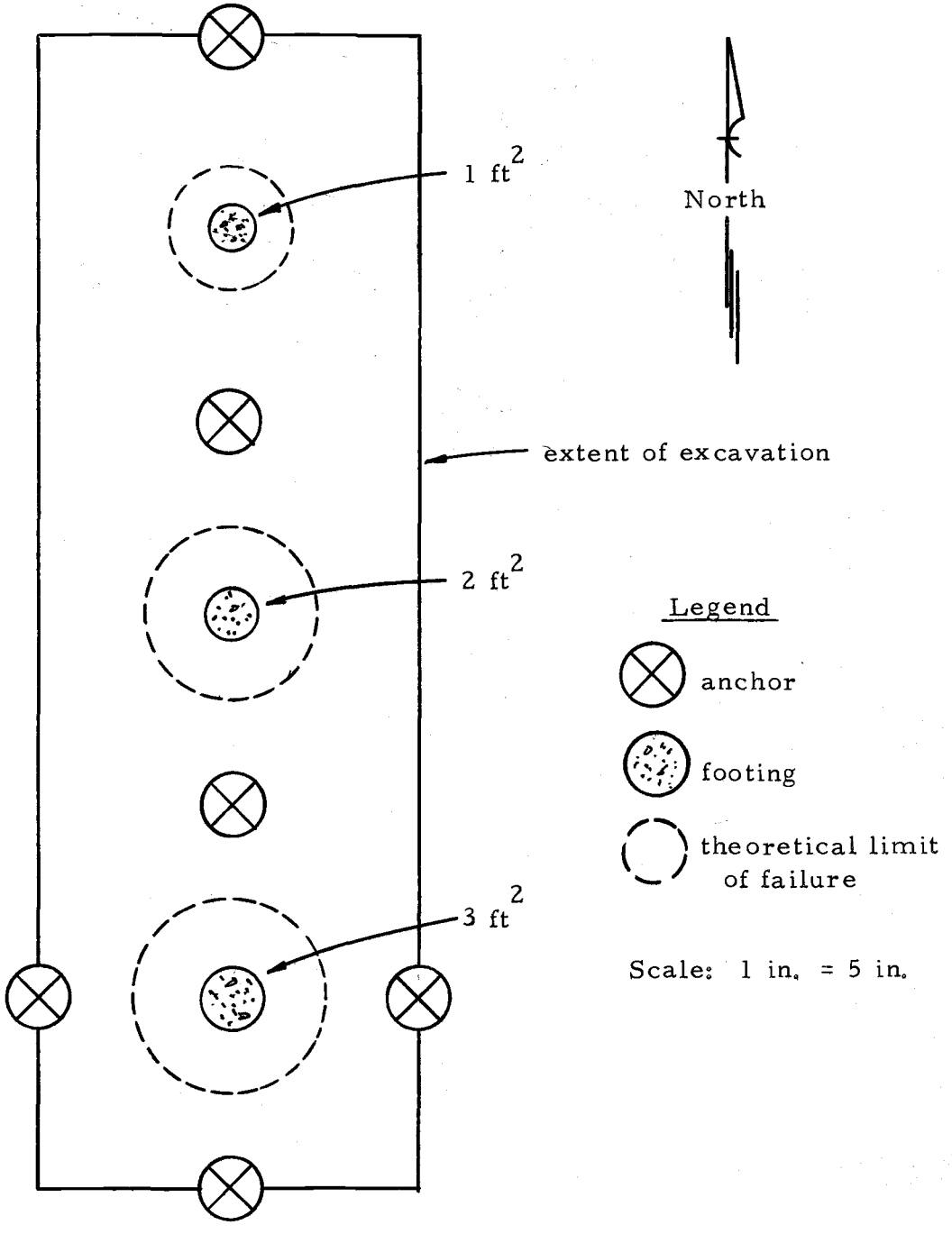

Figure 4. Test Site Layout.

Circular footings of 1, 2, and 3 square foot area were formed and "cast in place" in a pit excavated at the site location. The extent of the excavation and the location of the anchors were selected so that neither surcharge nor anchors would interfere with the failure surface of any test footing.

A 30 ton capacity hydraulic jack was used to load the footings. This jack was fitted with two pumps, a large pump for rapid movement of the jack ram and a small pump for slow controlled movement. A pressure gage connected to the jack measured load directly in thousand pound increments. This gage was only used for approximate control in applying and maintaining a constant load. Actual load measurements were made with a 50,000 pound capacity Strainsert flat load cell placed between the truss and the jack. Strain of the load cell was measured in microinches per inch on a four arm bridge strain indicator. Strain, as measured on the strain indicator, was calibrated against load applied to the cell in a compression testing machine. This system permitted measuring the load with an accuracy of about 12 pounds.

Load was applied from the jack to the footings through a ball and socket loading head so that any inclination in the truss would not affect the footing.

Three dial type extensometers were fixed to a steel ring suspended over the test footing from two reference beams. The

extensometers were sensitive to 0.001 inch and had a total range of one inch. The tips of the extensometers rested on the surface of the footing and were spaced at equal intervals around the edge of the footing as shown in Figure 5. By comparing settlements for each of the three gages over a given period of time it was possible to observe tipping of the footing before it was visible to the eye.

Procedure

Load tests were planned in accordance with ASTM D1194-72 (1). The load was applied to the test footings in increments equal to 10 percent of the estimated ultimate bearing capacity. The load applied to the footing was controlled by monitoring the strain indicator. The strain indicator was set at a strain calculated to be equal to the desired load; the strain indicator balance was then maintained by controlling the pressure on the jack with the small hand pump. With practice, it was not difficult to maintain the desired load. The load cell was quite sensitive to temperature so that the initial calibration of strain on the load cell was corrected for temperature by adjusting the initial strain reading.

ASTM suggests leaving a load increment on for at least 15 minutes or for a longer period until settlement ceases or becomes uniform. The first few load increments were left on for 25 minutes. Subsequent loading periods were 15 minutes. Examination of load

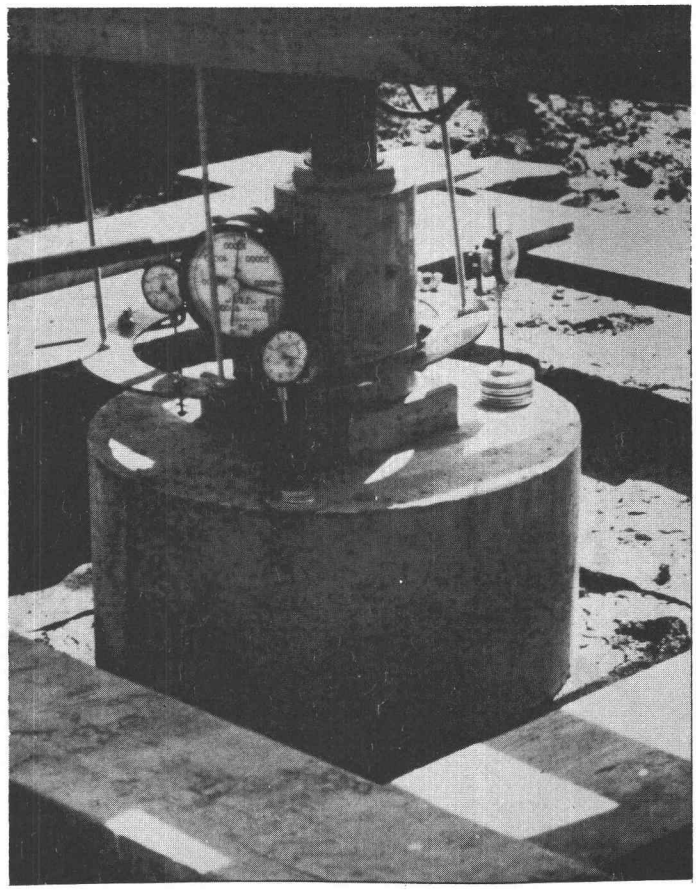

Figure 5. Dial Gage Extensometer Installation.

versus log time curves revealed for loads less than the ultimate bearing capacity, settlement had reached a uniform rate before 15 minutes of loading; however, at load increments above the ultimate bearing capacity, settlement did not reach a uniform rate even after 25 minutes.

Dial gage extensometers were used to measure settlement. The dial gages and their installation are described in the apparatus section. Two persons were required to perform the load tests. One read the dial gages and pumped the jack while the other watched the strain indicator and recorded the dial gage readings at various times after initial loading. Dial gage readings were recorded at 2, 5, and 15 minutes after the load was applied.

The weight of each footing and the load cell, jack and loading head were added to the load measured by the strain indicator to calculate the total load acting on the soil beneath the footings.

Results

The results of the three load tests performed in this study are presented in Figures 6, 7, and 8 as load versus settlement curves. These curves were plotted using load measured with the load cell plus the weight of the footing and loading apparatus versus settlement recorded by the extensometer showing the largest settlement. All extensometers recorded nearly the same settlement at loads below

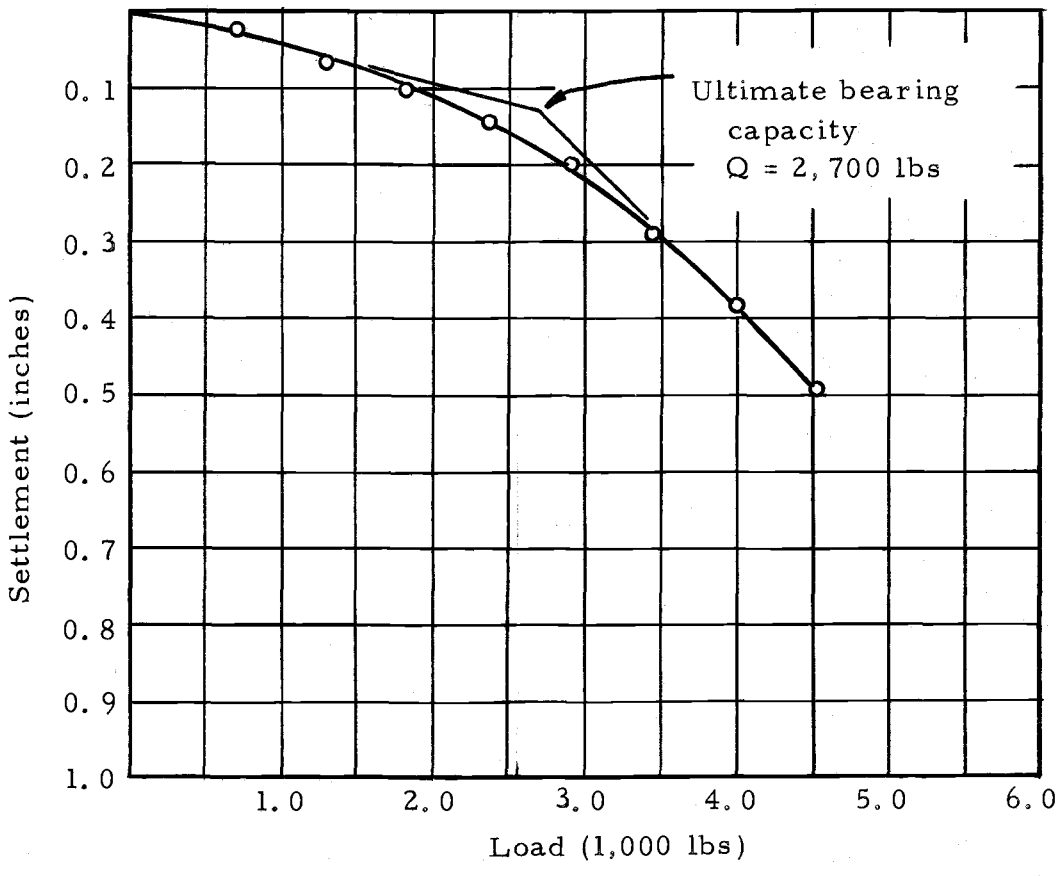

Figure 6. Load-Settlement Curve (1 ft^2 circular footing).

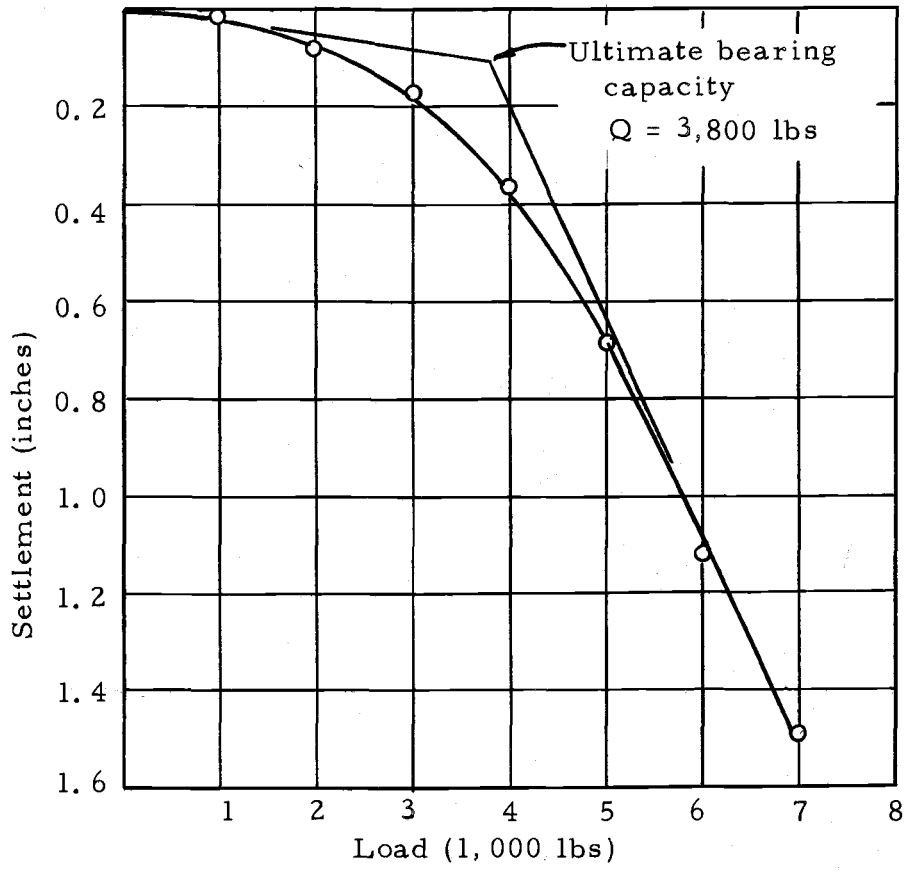

Figure 7. Load-Settlement Curve (2 ft^2 circular footing).

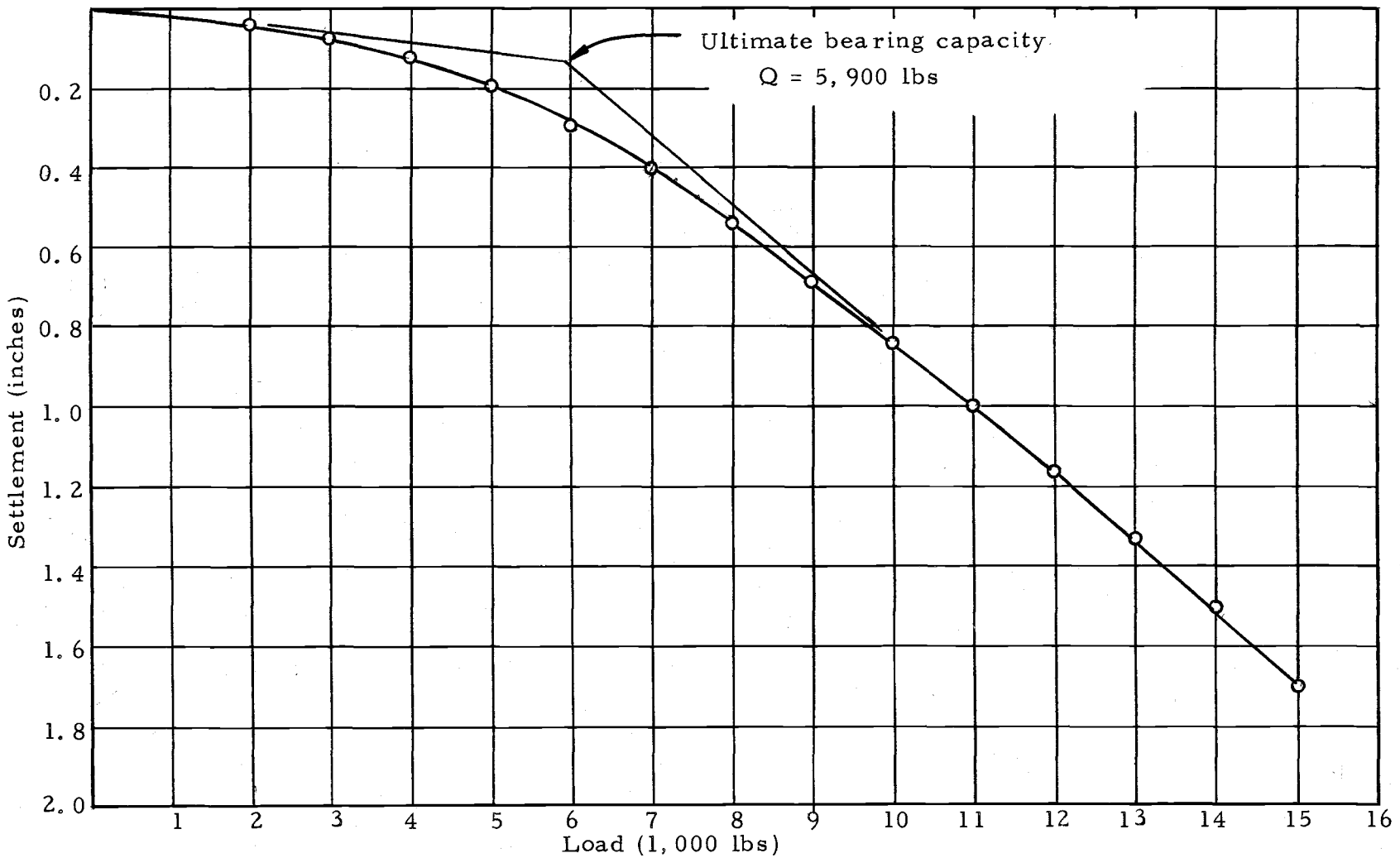

Figure 8. Load-Settlement Curve (3 ft^2 circular footing).

the ultimate bearing capacity; at loads above the ultimate bearing capacity, one extensometer began recording larger settlements, indicating tipping of the footing. When a footing became inclined more than two or three degrees from the horizontal, the load test was ended.

Figure 9 presents average footing contact pressure versus settlement for each of the three load tests.

Figure 10 shows the relationship between average footing contact pressure and the settlement recorded for the last five minutes of each loading period. This diagram represents a technique developed by Housel (7) for evaluating the ultimate bearing capacity from load test data on cohesive soils.

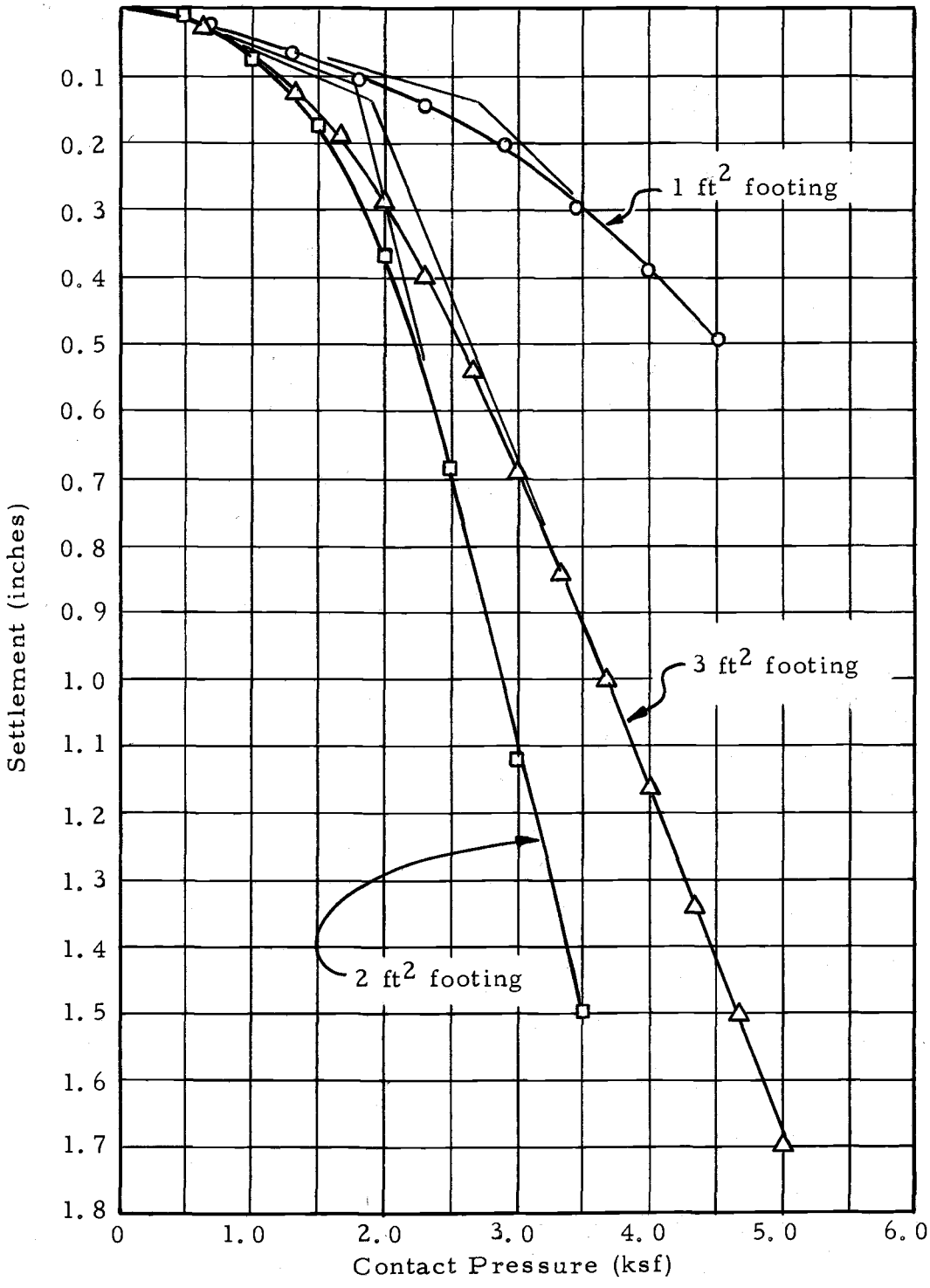

Figure 9. Comparison of Average Footing Contact Pressure versus Settlement for Various Footing Areas.

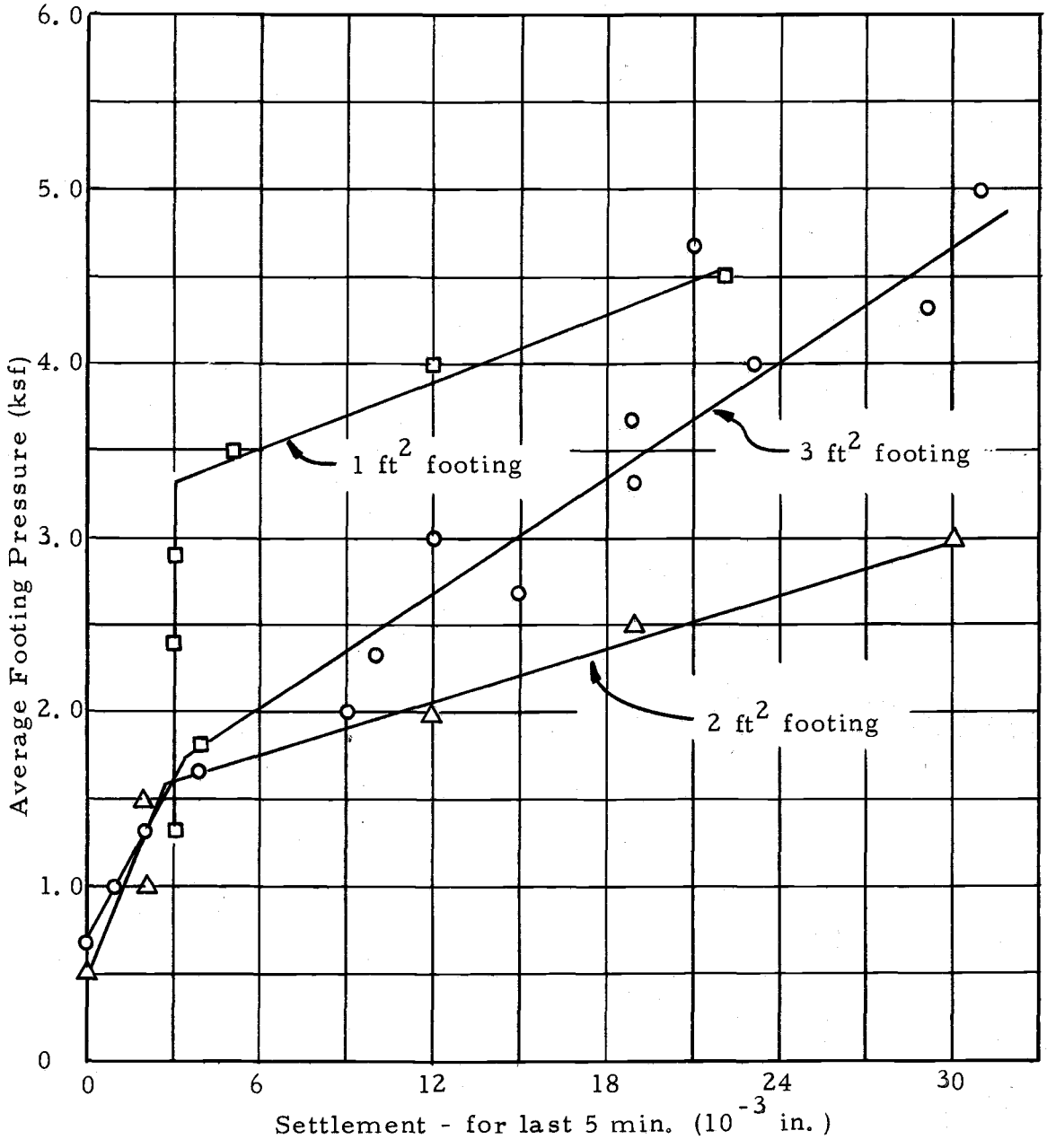

Figure 10. Average Footing Contact Pressure versus Settlement in the Last 5 Minutes.

VI. SOIL PROPERTIES

Soil Testing

Atterberg limits were performed on representative samples from the load test site. The procedure outlined by Lambe (9) was followed.

All other laboratory testing was performed on samples taken from three Shelby tubes. The Shelby tubes were driven into the bottom of the test pit using an eight pound sledge hammer and a Douglas-fir cushion block. The Shelby tubes were driven to a depth of 15 inches below the bottom of the test pit which was estimated to be the depth of the failure surface for the largest footing.

Torvane and pocket penetrometer measurements were made at various levels in each Shelby tube. Several measurements were made at each level to determine local variations.

Laboratory vane tests were performed on the samples while they were still in the Shelby tube. Tests were repeated for various levels in the Shelby tube sample. The vane penetrated the sample to a depth of one inch and was rotated at a rate of six degrees per minute.

Unconfined compression tests were run on two specimens which were extruded from a Shelby tube and trimmed to 1.4 inches diameter

by 2.8 inches high in a trimming frame. It was extremely difficult to trim these samples as they contained roots and the soil consistency was friable. The sample trimming operation caused significant disturbance to these specimens. The tests were performed at one percent strain per minute. Vertical cracks appeared in both specimens just before the failure load was reached.

Because of the difficulties encountered with trimming specimens for the unconfined compression test, further strength tests were performed on samples extruded from the Shelby tube and mitered to length without trimming to a smaller diameter. Unconsolidated, undrained triaxial tests were performed on these samples. A cell pressure of two pounds per square inch was calculated to represent the in situ stress of these specimens. It was difficult to maintain cell pressure at this low value with the pressure regulator in the system. At no time did the cell pressure reach as high as five pounds per square inch, but the cell pressure may have dropped as low as one-half pound per square inch during the tests. These tests were performed at a controlled strain rate of one percent per minute.

Consolidation testing was performed so that the stress history of the soil could be determined and a value for permeability could be back calculated. Consolidation was measured for 1/8, 1/4, 1/2, 1, 2, 4, and 8 tons per square foot loads. The sample was rebounded to 2 and then 1/2 ton per square foot load. Complete elapsed time

versus dial reading data were only taken for the one-half ton loading. All other consolidations were taken as the compression after 12 hours.

Results

A description of the soil profile at the test site and natural water content, liquid limit, and plastic limit of each soil unit is given in Figure 11. The unified soil classifications are shown in parentheses in this figure.

Figure 12 shows the location of Shelby tube samples in the test pit. Pocket penetrometer soil strength values are shown to indicate the variations at the site. The position of strength measurements are also indicated. Figure 12 indicates a trend towards increased, undrained cohesive strength near the small footing.

A summary of undrained cohesion, c_u, as determined by laboratory strength testing, is presented in Table 1. Torvane and pocket penetrometer measurements are included in this table so that they can be compared to the laboratory strength values.

A comparison of average undrained cohesions for the various tests shows the undrained shear strength measured by the pocket penetrometer is at least twice the values determined with the other strength testing apparatus. Also, the unconfined compression test results are very questionable since sample trimming caused significant disturbance to the test specimens.

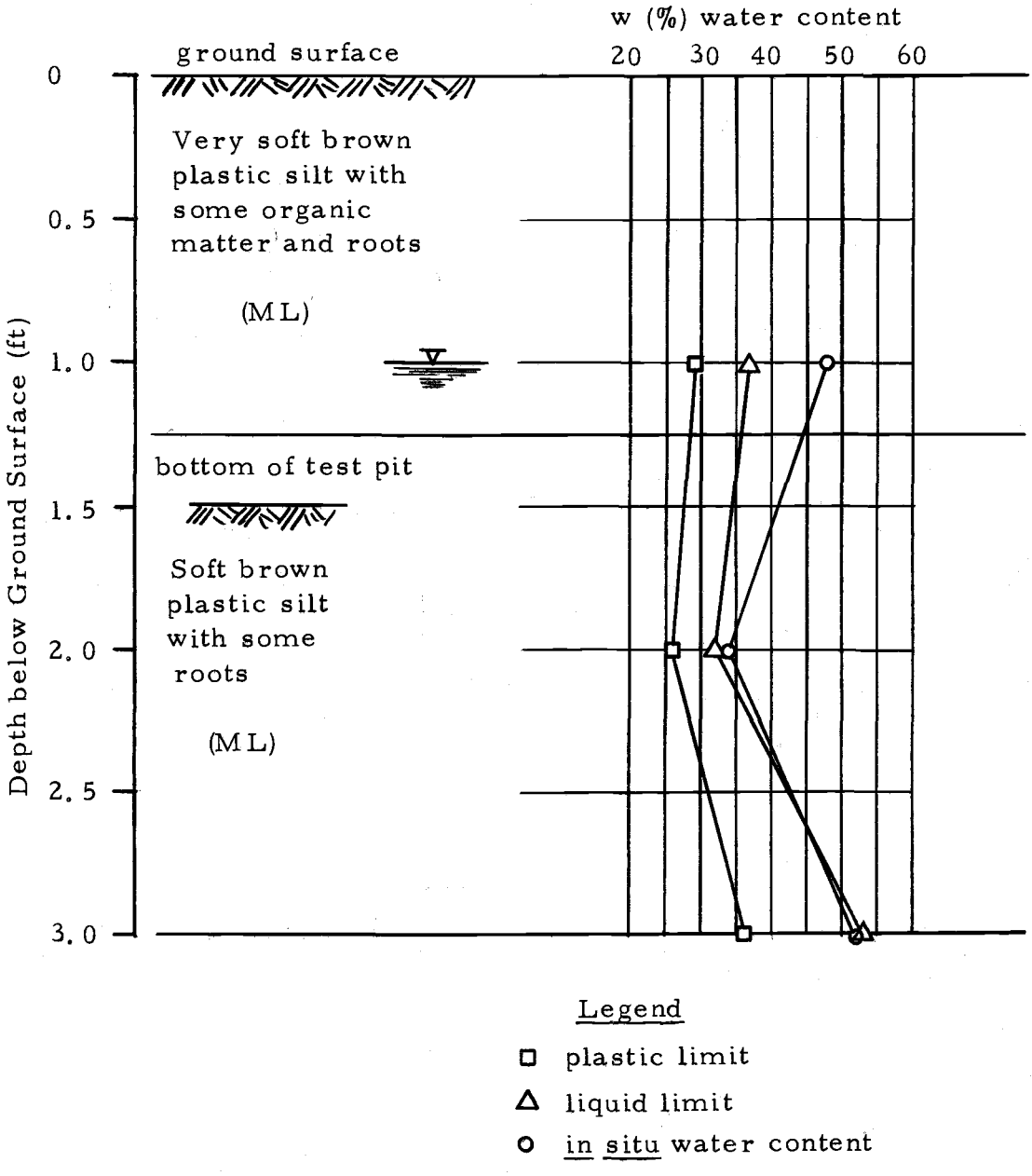

Figure 11. Soil Profile at Test Site.

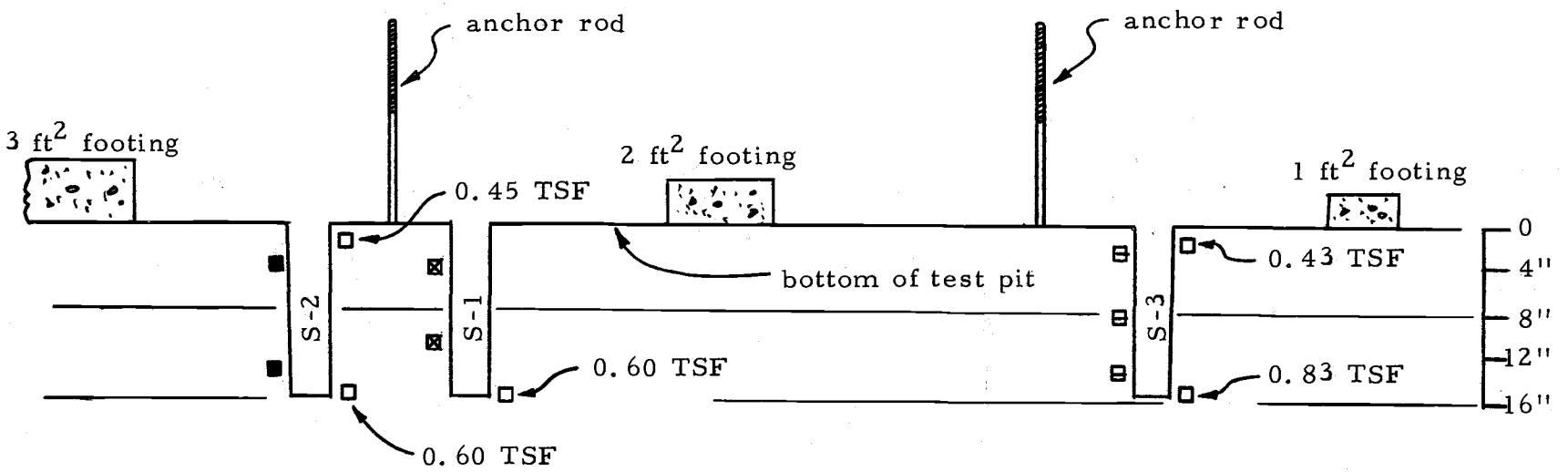

Note: Horizontal distances not to scale

Legend

- pocket penetrometer
- unconfined compression test
- laboratory vane
- unconsolidated-undrained triaxial

Figure 12. Location of Strength Tests Performed on Samples from the Test Site.

Table 1. Summary of Undrained Soil Strength.

Type of Test	No. of Tests	Cohesion (c_u), TSF		
		Maximum	Minimum	Average
Torvane	5	0.36	0.13	0.25
Pocket Penetrometer	5	0.83	0.43	0.61
Laboratory Vane	3	0.38	0.29	0.33
Unconfined Compression	2	0.18	0.13	0.16
Unconsolidated-Undrained Triaxial	2	0.22	0.20	0.21

A void ratio versus log of effective stress curve was plotted from consolidation testing data and presented as Figure 13. Examination of this curve shows the silt of this study is over-consolidated. The preconsolidation pressure was estimated to be 0.94 tons per square foot by the Casagrande graphical construction.

A dial reading versus log time curve for the one-half ton per square foot load is presented in Figure 14. One hundred percent of primary consolidation was estimated to have taken place in 33 minutes.

The coefficient of permeability was calculated to be 1.26×10^{-4} centimeters per second for the void ratio corresponding to the one-half tons per square foot load. The coefficient of permeability determined from consolidation test data is dependent upon the validity

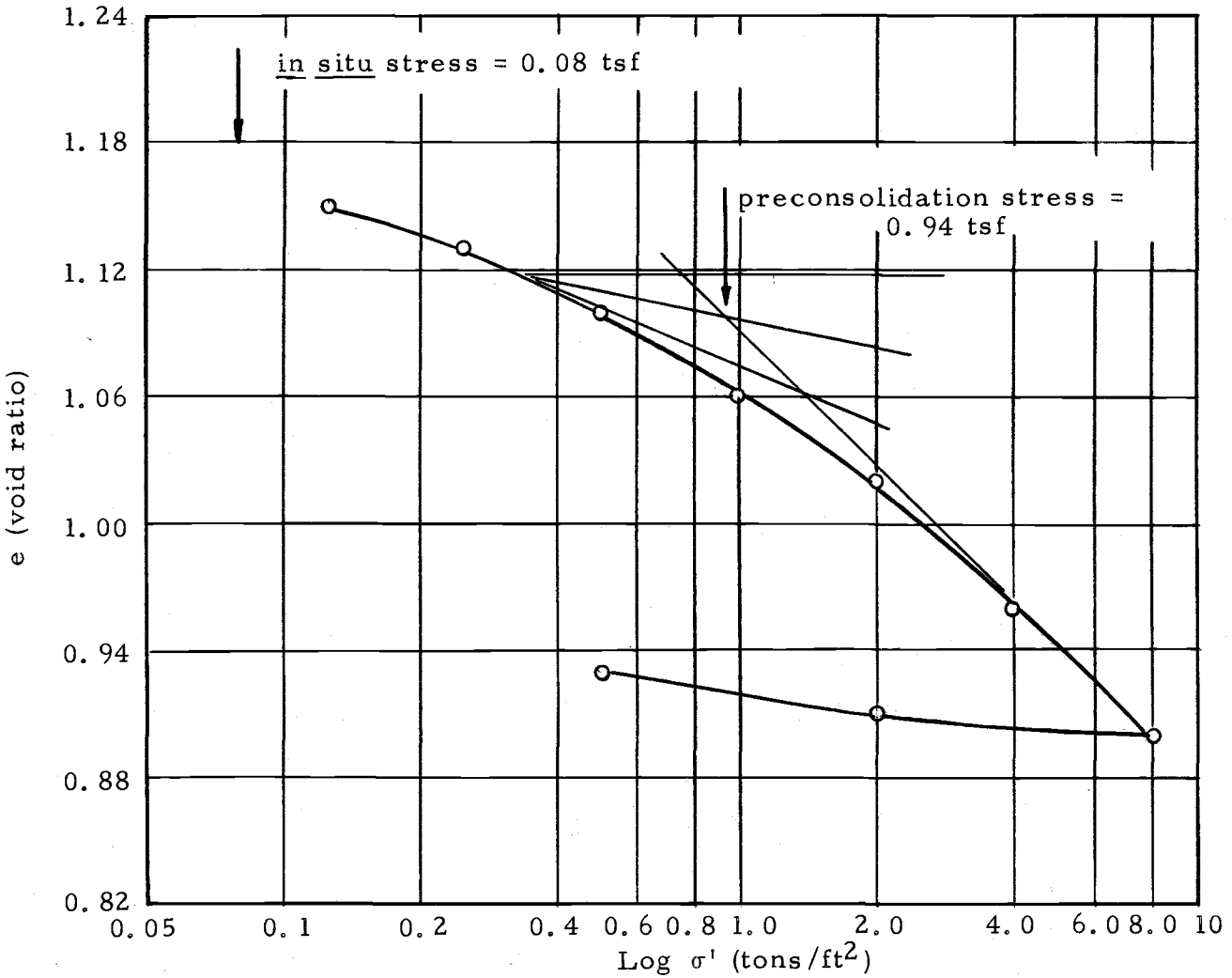

Figure 13. Void Ratio versus Log Effective Stress.

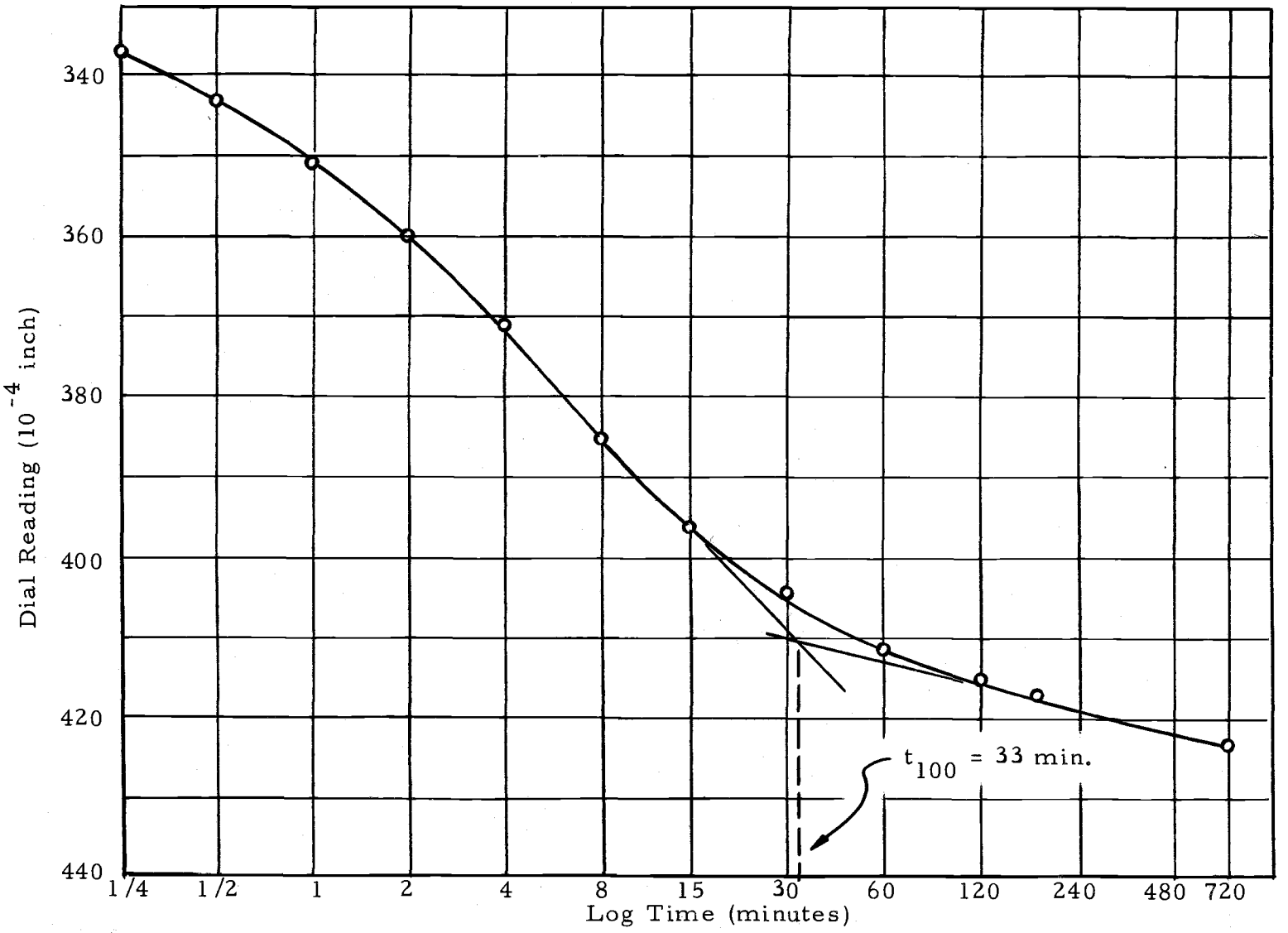

Figure 14. Dial Reading versus Log Time Curve (1/2 TSF load).

of the Terzaghi one-dimensional consolidation equation; therefore, the coefficient of permeability calculated should be regarded as indicating an order of magnitude rather than an exact value.

VII. INTERPRETATION OF RESULTS

Soil properties determined from Atterberg limits and consolidation testing are discussed first with the objective of establishing that the load testing was performed on a plastic silt of moderate permeability. Secondly, load test data are evaluated to determine an ultimate bearing capacity for each of the three footings. Thirdly, the laboratory undrained shear strength values are analyzed to provide a "best" estimate of the undrained shear strength of the soil beneath the test footings. Finally, the bearing capacity determined from load tests is compared to the bearing capacity calculated by the various bearing capacity equations using the undrained soil strength determined from laboratory testing.

Atterberg limits performed on the soil beneath the test pit confirm that this soil is a plstic silt of moderate to low compressibility. This soil classifies ML according to the Unified Soil Classification system.

A coefficient of permeability of 1.26×10^{-4} centimeters per second was calculated from consolidation test data. According to Wu (20), the coefficient of permeability for silts ranges from 10^{-3} to 10^{-6} centimeters per second. The soil considered by this study is clearly between the extremes of a free draining sand and an impervious clay.

The simplest method of determining ultimate bearing capacity from load test data is to plot load versus settlement curves and extend the initial straight line portion forward and the final straight line portion backward. The intersection of these lines is taken as the ultimate bearing capacity. This procedure was followed in Figures 6, 7, and 8. The bearing capacities determined with this procedure are not distinct because the initial portions of the load versus settlement curves are not straight. Judgment was employed in estimating the point where curvature of the initial portion became significant. A tangent was drawn from the initial portion of the curve where curvature was small. It was easier to determine where the final portion of the curves approached straight lines. By trying various tangents, which reasonably modeled an initial straight line portion, it was possible to determine a range of ultimate bearing capacities plus or minus five percent of the values given in Figures 6, 7, and 8.

Housel (7) proposed a method for evaluating ultimate bearing capacity from load settlement curves where an initial straight line portion is not clearly defined. He suggested plotting average footing pressure versus settlement in the last 30 minutes of a one hour loading period. A sharp break in slope is then observed at the ultimate bearing capacity. The loading period used with the load tests performed in this study was 15 minutes. Footing pressure was plotted against settlement in the last five minutes in an attempt to fit the load

test data into the Housel procedure. Figure 10 shows these curves for the three footings tested. A large change in slope is observed at what may be taken as the ultimate bearing capacity for each of the three footings. Table 2 is a comparison between the bearing capacities determined with the modified Housel procedure and those determined from the conventional procedure. It may be significant that for the two and three square foot footings, the bearing capacities determined from the modified Housel procedure agree well with the bearing capacities determined from the intersections of straight line portions of the load settlement curves. Because of the short loading period, Housel's method may not be applicable to these tests.

Table 2. Comparison of Methods of Determining Ultimate Bearing Capacity from Load Test Data.

Footing Size (ft^2)	Ultimate Bearing Capacity (psf)	
	Housel Procedure	Conventional Procedure
1	3,300	2,700
2	1,600	1,900
3	1,730	1,967

The one square foot footing is peculiar in that its unit bearing capacity is significantly larger than those of the other footings. There are two possible explanations for the increased bearing capacity of the smaller footing. First, the soil beneath the small footing might have had a greater shear strength than the soil affected

by the larger footings. Secondly, partial drainage of excess pore-water pressure might have occurred. Drainage would be greatest for the smallest footing due to a shorter drainage path. If partial drainage was responsible for the increase, then the two foot square footing should have a larger bearing capacity than the three foot square footing. The larger footings have nearly equal bearing capacities, suggesting that no porewater drainage occurred. Most probably, the smaller footing was affected by local variations in soil strength. The pocket penetrometer, which is the only test performed on specimens from all three Shelby tubes, shows a greater relative strength near the smaller footing. The ratio of the shear strengths near the small footing to the shear strengths between the two larger footings as determined with the pocket penetrometer is very nearly the same as the ratio of the ultimate bearing capacity of the small footing to the ultimate bearing capacity of the larger footings.

A large variation is observed in the undrained cohesive strengths determined with the Torvane and pocket penetrometer (see Table 1). Both these strength measuring devices test only a small volume of soil, and being handheld, are subject to considerable error. The unconfined compression test and the unconsolidated-undrained triaxial test test larger soil volumes and should be less subject to local strength variations. Unfortunately, the unconfined compression test data collected are not reliable. The difficulties encountered in

trimming test specimens from this soil caused significant disturbance. Several specimens were trimmed in order to obtain two specimens without visible cracks. The unconsolidated-undrained triaxial test and the laboratory vane test data best represent the soil strength for this investigation.

The unconsolidated-undrained triaxial tests were performed on specimens extruded from Shelby tube number two. The average undrained cohesion measured for these specimens was 420 pounds per square foot. Shelby tube number two was driven into the soil at the bottom of the test pit approximately halfway between the two larger footings (see Figure 12). The laboratory vane tests were performed on soil samples at various levels in Shelby tube number three. This sample was taken from an area in the test pit near the small footing. The average undrained cohesion determined with the laboratory vane apparatus was 660 pounds per square foot. The larger undrained cohesion determined with the laboratory vane is consistent with the trend of pocket penetration values which increase near the small footing. All of the undrained strength data show the soil in the test area was soft.

According to Housel (7) both the unconsolidated-undrained triaxial test and the laboratory vane test are reliable methods for determining cohesive strength. The unconsolidated-undrained triaxial tests were performed at the same strain rate as the

unconfined compression tests, the only difference was that planes of weakness were held closed by cell pressure. For intact specimens the unconsolidated triaxial test and the unconfined compression test should yield essentially the same results. Housel (7) states that the laboratory vane test and the unconfined compression test should provide comparable undrained shear strengths. In a study performed by Goughnour and Sallberg (5) it was discovered that the ratio of soil strength determined from the laboratory vane test to the soil strength determined from the unconfined compression test varied with the plasticity index. They found a ratio of eight-tenths for soils of the same plasticity as the plastic silt considered in this study. It appears that the undrained soil strength determined from the laboratory vane test might be a low estimate of the unconsolidated-undrained triaxial test soil strength for the same soil sample. In any case, the trend towards a higher strength near the small footing appears clear.

The shape of the load-settlement curves (Figures 6, 7, and 8) indicates that the footings failed under local shear failure conditions. Using Terzaghi's empirical reduction to the undrained cohesion for local shear failure, and the values of undrained cohesion from the unconsolidated-undrained triaxial tests and the laboratory vane tests and equations 6a, 6b, and 6c the ultimate bearing capacities are calculated as follows:

Terzaghi $q_D = 6.17 \times 2/3 \times 420$ psf = 1727 psf

Meyerhof $q_D = 6.18 \times 2/3 \times 420$ psf = 1730 psf

Hansen $q_D = 6.68 \times 2/3 \times 420$ psf = 1870 psf

and

Terzaghi $q_D = 6.17 \times 2/3 \times 660$ psf = 2715 psf

Meyerhof $q_D = 6.18 \times 2/3 \times 660$ psf = 2719 psf

Hansen $q_D = 6.68 \times 2/3 \times 660$ psf = 2939 psf

If the laboratory vane test data for undrained cohesion is taken as representative of the soil strength beneath the one square foot footing and the unconsolidated-undrained triaxial data are taken as representative of the two larger footings, the soil bearing capacity measured by the load tests can be compared to calculated bearing capacities. Table 3 presents this comparison between measured and calculated bearing capacities.

Table 3. Calculated Bearing Capacity Compared to Load Test Results.

Footing Size (ft^2)	Calculated Bearing Capacity (psf)			Load Test Results (psf)
	Terzaghi	Meyerhof	Hansen	
1	2,715	2,719	2,939	2,700
2	1,727	1,730	1,870	1,900
3	1,727	1,730	1,870	1,967

The greatest difference between measured and calculated bearing capacity is 12 percent for the largest footing. The one and

two square foot footings show a maximum of nine percent variation between measured and calculated values. Considering the local shear failure correction to the bearing capacity equations is only an approximation, the observed correlation is remarkably good.

It is apparent that the $\phi = 0$ analysis is applicable to this soil for the rate of load application used. The load test on each footing was accomplished in approximately four hours. How well these load tests model the bearing capacity of an actual foundation when the load is applied over a construction period is an unanswered question. For an eight foot square footing, the load would have to be applied in approximately four days to duplicate load test drainage conditions, assuming the drainage path is directly proportional to the footing diameter. Sixty days is probably a more appropriate estimate of the construction period for a building which would require an eight foot square footing. To model this loading condition, the failure load should be applied over a 24 hour period.

It is important to visualize the actual soil-foundation system and the rate at which load will be applied when bearing capacity equations are used to design footing contact pressure. If bearing capacity were calculated using the $\phi = 0$ analysis without the local shear failure reduction, the bearing capacity would have been greatly over-estimated. If an inexperienced or careless engineer calculated a bearing capacity from the average pocket penetrometer undrained

shear strength and did not make the reduction for local failure, the bearing capacity would have been over-estimated by 400 percent and a calculated factor of safety of three would actually be less than one.

VIII. CONCLUSIONS

For the plastic silt investigated in this study, the ultimate bearing capacities determined from load tests are best modeled by the $\phi = 0$ analysis with the Terzaghi reduction for the local shear failure condition. In this case the Terzaghi, Meyerhof, and Hansen analyses all provide good correlation with load test results. If the load were applied to the test footings at a slower rate, then the $\phi = 0$ analysis might be overly conservative; however, ordinarily the rate of construction is not well defined and the $\phi = 0$ analysis provides a satisfactory design procedure.

Plastic silts cover a large range in permeability and consequently, the conclusions suggested by this study should not be extended to plastic silts in general. There is a need for further study of the bearing capacities of plastic silts. This is particularly true for those of lower plasticity and/or where construction rate is to be modeled with load tests.

BIBLIOGRAPHY

1. American Society for Testing Materials, Annual Book of Standards, Part 11, Philadelphia, 1972. pp. 395-397.

2. Berfelt, A., "Loading Tests on Clay," Geotechnique, Vol. 6, London, 1956. pp. 15-31.

3. Bowles, Joseph E., Foundation Analysis and Design, New York, McGraw-Hill, 1968. pp. 47-53.

4. Brown, Philip P. and James R. Libby, Oregon State College Foundation Investigation, (Corvallis), 1950. 60 pp.

5. Goughnour, R. D. and J. R. Sallberg, "Evaluation of the Laboratory Vane Shear Test," Highway Research Record No. 48, Highway Research Board, 1964. pp. 19-33.

6. Helenelund, K. V., Investigation on the Bearing Capacity and Engineering Properties of Silt, The State Institute for Technical Research, Finland, 1965. 121 pp.

7. Housel, William S., "Dynamic and Static Resistance of Cohesive Soil," Special Technical Publication 254, American Society for Testing Materials, 1959. pp. 18-22.

8. Konder, Robert L. and Raymond J. Krizek, "Correlation of Load Bearing Tests on Soils," Proceedings of the 41st Annual Meeting, Highway Research Board, 1962. pp. 557-590.

9. Lambe, T. William, Soil Testing for Engineers, New York, Wiley, 1951. pp. 22-28.

10. Larkin, Lawerence A., "Theoretical Bearing Capacity of Very Shallow Footings," Journal of the Soil Mechanics and Foundations Division, American Society of Civil Engineers, SM6, 1968. pp. 1347-1357.

11. Means, R. E. and J. V. Parcher, Physical Properties of Soils, Columbus, Merrill, 1963. pp. 273-274.

12. Meyerhof, G. G., "The Ultimate Bearing Capacity of Foundations," Geotechnique, Vol. 2, No. 4, 1951. pp. 301-333.

13. Milovic, D. M., "Comparison between the Calculated and Experimental Bearing Capacity," Proceedings of the 6th International Conference on Soil Mechanics and Foundation Engineering, Vol. 2, Montreal, 1965. pp. 142-144.

14. Peck, Ralph B., Walter E. Hanson and Thomas H. Thornburn, Foundation Engineering, Second edition, New York, Wiley, 1974. pp. 272-273.

15. Skempton, A. W., "The Bearing Capacity of Clays," Proceedings, Building Research Congress, Vol. 1, London, 1951. pp. 180-189.

16. Sowers, G. F., "Shallow Foundations," in: Foundation Engineering, ed. by G. A. Leonards, New York, McGraw-Hill, 1962. pp. 538-544.

17. Terzaghi, Karl, Theoretical Soil Mechanics, New York, Wiley, 1943. pp. 53-56, 118-134.

18. Terzaghi, Karl and Ralph B. Peck, Soil Mechanics in Engineering Practice, second edition, New York, Wiley, 1968. pp. 217-224, 502-504.

19. Tschebortarioff, Gregory P., Foundations, Retaining and Earth Structures, second edition, New York, McGraw-Hill, 1973. pp. 132-139.

20. Wu, T. H., Soil Mechanics, Boston, Allyn and Bacon, 1966. pp. 36-37.